

Note

**Alkyl-substituted cucurbit[6]uril bridged #-cyclodextrin  
dimer mediated intramolecular FRET behavior**

Fang-Fang Shen, Ying-Ming Zhang, Xian-Yin Dai, Hao-Yang Zhang, and Yu Liu

*J. Org. Chem.*, **Just Accepted Manuscript** • DOI: 10.1021/acs.joc.9b03513 • Publication Date (Web): 08 Apr 2020

Downloaded from [pubs.acs.org](https://pubs.acs.org) on April 10, 2020

**Just Accepted**

“Just Accepted” manuscripts have been peer-reviewed and accepted for publication. They are posted online prior to technical editing, formatting for publication and author proofing. The American Chemical Society provides “Just Accepted” as a service to the research community to expedite the dissemination of scientific material as soon as possible after acceptance. “Just Accepted” manuscripts appear in full in PDF format accompanied by an HTML abstract. “Just Accepted” manuscripts have been fully peer reviewed, but should not be considered the official version of record. They are citable by the Digital Object Identifier (DOI®). “Just Accepted” is an optional service offered to authors. Therefore, the “Just Accepted” Web site may not include all articles that will be published in the journal. After a manuscript is technically edited and formatted, it will be removed from the “Just Accepted” Web site and published as an ASAP article. Note that technical editing may introduce minor changes to the manuscript text and/or graphics which could affect content, and all legal disclaimers and ethical guidelines that apply to the journal pertain. ACS cannot be held responsible for errors or consequences arising from the use of information contained in these “Just Accepted” manuscripts.

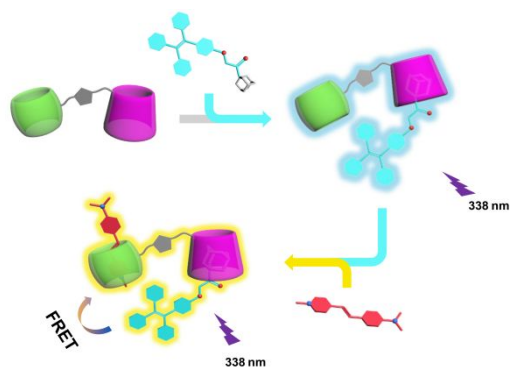
1  
2  
3  
4 **Alkyl-substituted cucurbit[6]uril bridged  $\beta$ -cyclodextrin dimer**  
5  
6 **mediated intramolecular FRET behavior**  
7  
8  
9

10  
11 Fang-Fang Shen, Ying-Ming Zhang, Xian-Yin Dai, Hao-Yang Zhang, Yu Liu\*  
12  
13

14  
15  
16  
17  
18  
19 College of Chemistry, State Key Laboratory of Elemento-Organic Chemistry, Nankai  
20  
21 University, Tianjin 300071, China  
22  
23  
24  
25

26  
27 yuliu@nankai.edu.cn  
28  
29  
30  
31  
32  
33  
34  
35  
36  
37  
38  
39  
40  
41  
42  
43  
44  
45  
46  
47  
48  
49  
50  
51  
52  
53  
54  
55  
56  
57  
58  
59  
60

## Graphic Abstract



**Abstract**

A novel triazolyl bridged cucurbituril (CB)-cyclodextrin (CD) dimer was synthesized via click reaction of mono-propargyl modified octamethylcucurbit[6]uril and mono-6-azido- $\beta$ -cyclodextrin. Moreover, it could form stable supramolecular inclusion complexes possessing efficient fluorescence resonance energy transfer, which was benefit from that CD and CB can bind amantadine- and pyridinium-containing fluorophores simultaneously. The supramolecular inclusion complex behaviors were investigated by NMR spectroscopy, UV-vis absorption and fluorescence spectroscopy.

1  
2  
3  
4 Cucurbit[*n*]urils (CB[*n*]s, *n* = 5–8, 10, 14) are a class of synthetic macrocyclic host  
5  
6 molecules consisting of *n* glycoluril units with a hydrophobic cavity and two identical  
7  
8 carbonyl-fringed portals.<sup>1</sup> Although (CB[*n*]s) are potentially used as a type of host  
9  
10 receptors<sup>2</sup>, their practical applications in chemistry, biology and material areas have  
11  
12 been limited, probably due to the insufficient solubility and the difficulty of  
13  
14 introducing functional groups on their surfaces. Since the discovery of the first fully  
15  
16 alkyl-substituted CB[5], decamethylcucurbit[5]uril, in 1992,<sup>3</sup> a series of fully and  
17  
18 partially alkyl-substituted cucurbit[*n*]urils (SCB[*n*]s) derivatives have been reported  
19  
20 successively.<sup>4–6</sup> The physical and chemical properties of alkyl-substituted CB[*n*]s have  
21  
22 been changed, such as cavity size, shape and electron cloud density of carbonyl  
23  
24 oxygen atoms, which increased the solubility in common solvents and produced other  
25  
26 special functional properties. The introduction of functional groups on skeletons of  
27  
28 CB[*n*]s has been a huge challenge in CB[*n*] chemistry due to chemical stability of  
29  
30 CB[*n*]s. In 2003, Kim and co-workers firstly prepared a series of CB[*n*] derivatives,  
31  
32 hydroxy-substituted (HO)<sub>2*n*</sub>CB[*n*]s, by simple oxidation of the native CB[*n*]s with  
33  
34 K<sub>2</sub>S<sub>2</sub>O<sub>8</sub> in water,<sup>7</sup> and this served as a accelerator for the application of functionalized  
35  
36 CB[*n*]s in vesicles, polymers, nanomaterials, artificial ion channels, and so on.<sup>8–13</sup>  
37  
38 However, the yields for alkyl-substituted CB[*n*]s in this method was too low for  
39  
40 practical use. Until 2015, Bardelang and Ouari discovered a photochemical method by  
41  
42 UV and hydrogen peroxide to introduce a limited number of alcohol functional groups  
43  
44 on CB[*n*]s (*n* = 5, 6, 7, and 8).<sup>14</sup> Although they have made a correction of conversions  
45  
46 from 95–100% to 20–40%,<sup>15</sup> this method can be applied to other selected CB[*n*]s,  
47  
48  
49  
50  
51  
52  
53  
54  
55  
56  
57  
58  
59  
60

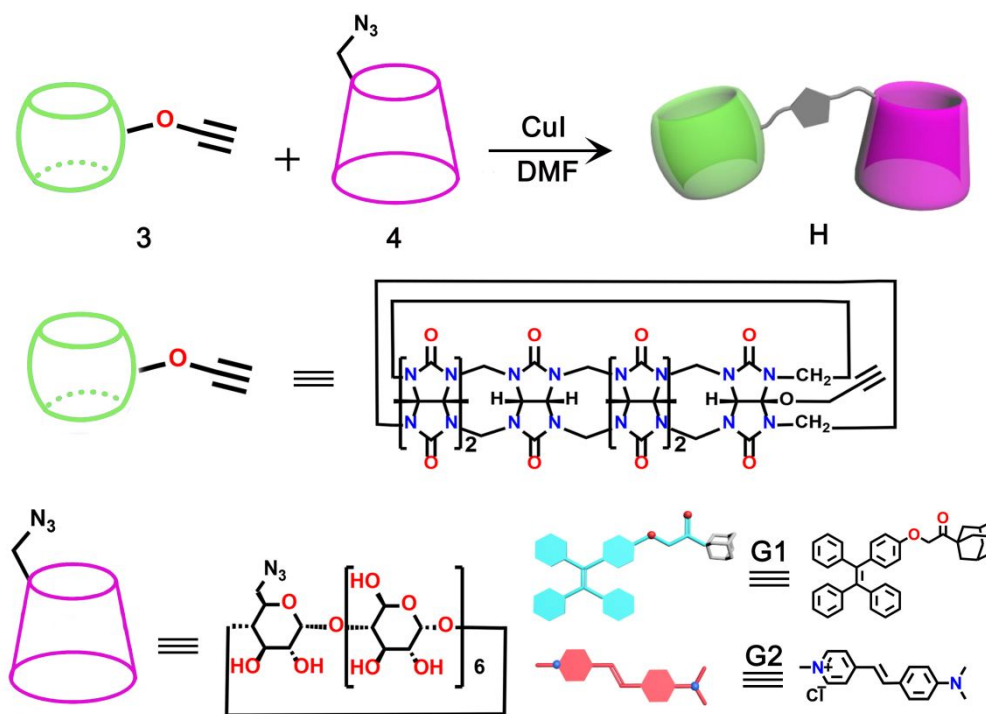
1  
2  
3  
4 including alkyl-substituted CB[n]s. However, the functionalization of  
5  
6 alkyl-substituted CB[n]s is still rarely reported.<sup>16,17</sup>  
7  
8

9 On the other hand, as one of very important photophysical properties, fluorescence  
10  
11 resonance energy transfer (FRET) is a research hotspot for scientists in miscellaneous  
12  
13 fields. The occurrence of a more effective FRET phenomenon requires some criteria.  
14  
15 That is, a FRET system includes at least two chromophores, the donor and the  
16  
17 acceptor, which should be located in close proximity and the fluorescence emission  
18  
19 spectrum of donor should sufficiently fall into the absorption spectrum of acceptor.  
20  
21  
22 However, there are still several defects in the constructing FRET materials, such as  
23  
24 the lack of controllability of covalently connected donor and acceptor, the insufficient  
25  
26 solubility in aqueous solution, and the weak interaction between independent  
27  
28 fluorophores. Remarkably, through flexible and controllable regulation of the  
29  
30 interaction between donor and acceptor pairs, the FRET systems constructed in the  
31  
32 form of supramolecular host–guest chemistry could serve as a promising tool to solve  
33  
34 these drawbacks. As a result, many interesting supramolecular FRET systems have  
35  
36 been constructed and applied in various fields.<sup>18</sup> For instance, Zhou and Yang  
37  
38 exhibited a acid/base-controllable FRET system by a host–guest complex between a  
39  
40 rhodamine B functionalized pillar[5]arene and cyano-modified boron  
41  
42 dipyrromethene.<sup>19</sup> Park and Kim reported a supramolecular nanosystem based on  
43  
44 the fusion assay of two different organelles using a novel host–guest pair,  
45  
46 cucurbit[7]uril-Cy3 and adamantane-Cy5 as a FRET pair.<sup>20</sup> Several FRET systems  
47  
48 were also constructed in our research group, using the strategy of supramolecular  
49  
50  
51  
52  
53  
54  
55  
56  
57  
58  
59  
60

1  
2  
3  
4 polymers based on host–guest complexation or in a nano-sized noncovalent  
5  
6 supramolecular assembly.<sup>21,22</sup> However, in a single supramolecular assembled entity,  
7  
8 the utilization of two different types of macrocyclic receptors to achieve efficient  
9  
10 FRET process still remains challenging.  
11  
12

13  
14 In order to study the binding and photophysical behaviors of functionalized SCB[*n*]s,  
15  
16 we utilized SCB[*n*]s possessing OH group at designated position to yield a special  
17  
18 oxidation product. Inspired by the complementary molecular binding behaviors of  
19  
20 CB[*n*]s and cyclodextrins (CDs).<sup>23</sup> In this work, we designed and synthesized a novel  
21  
22 macrocyclic dimer **H** (Figures S4–S6, Supporting Information) consisting of a  
23  
24 symmetrical octamethylcucurbituril (OMeCB[6]) and β-CD, in which two  
25  
26 macrocyclic molecules, (propargyl)<sub>1</sub>OMeCB[6] (Figures S1–S3, Supporting  
27  
28 Information) and mono-6-azido-β-CD was covalently conjugated via click reaction.  
29  
30 In our case, given that β-CD can incorporate neutral guest molecules possessing an  
31  
32 adamantyl end with high binding affinity, the adamantyl tetraphenylethylene (**G1**)  
33  
34 (Figures S7–S9, Supporting Information) was accordingly synthesized. Meanwhile,  
35  
36 OMeCB[6] is capable of encapsulating cationic guests in its hydrophobic cavity and  
37  
38 the binding constant between OMeCB[6] and  
39  
40 *trans*-4-[4-(dimethylamino)styryl]-1-methylpyridinium chloride (**G2**) can reach up to  
41  
42 10<sup>6</sup> M<sup>-1</sup> order of magnitude. Further spectroscopic studies have shown that H has the  
43  
44 larger binding affinity for these two guest molecules (**G1** and **G2**) than individual  
45  
46 macrocycle molecules (CB and CD moieties) (Scheme 1). Due to the superior  
47  
48 solubility of macrocyclic dimers in **H**, an intramolecular FRET system mediated by  
49  
50  
51  
52  
53  
54  
55  
56  
57  
58  
59  
60

the conjugation of CB with CD moieties was achieved in an aqueous solution, and the FRET efficiency was determined to be 70.3%.



**Scheme 1.** Schematic illustration of the structural formulas of **H**, **G1** and **G2** molecules.

To confirm the formation of the host–guest complexes between the OMeCB[6] moiety of **H** and **G2** as well as free OMeCB[6] and **G2**,  $^1\text{H}$  NMR spectroscopic titrations were first performed by using **G2** as a guest compound and free OMeCB[6] as a model host compound. As shown in Figure S10 (Supporting Information), upon the gradual addition of **G2**, the proton signals of the guest appeared to shift upfield ( $\Delta\delta = -0.22, -0.83, -0.09$ , for  $\text{H}_1, \text{H}_2, \text{H}_3$  respectively), suggesting that these protons of the guest were included in the cavity of the OMeCB[6] and were shielded by the

OMeCB[6]. In contrast, the signal of H<sub>4</sub>, H<sub>5</sub> moved downfield by 0.13 and 0.56 ppm, suggesting that these protons on the guest were excluded at the portals of the OMeCB[6]. Additionally, the NMR assignments were made through <sup>1</sup>H-<sup>1</sup>H COSY experiment (Figure S11, Supporting Information). Moreover, when adding 1.0 equiv. of **H** to **G2**, similar <sup>1</sup>H NMR complexation induced shifts occurs to protons of **G2** compared with OMeCB[6]/**G2** complex (Figure S12 Supporting Information), indicating that **H** and **G2** could form the same host-guest complex as OMeCB[6]/**G2** complex.

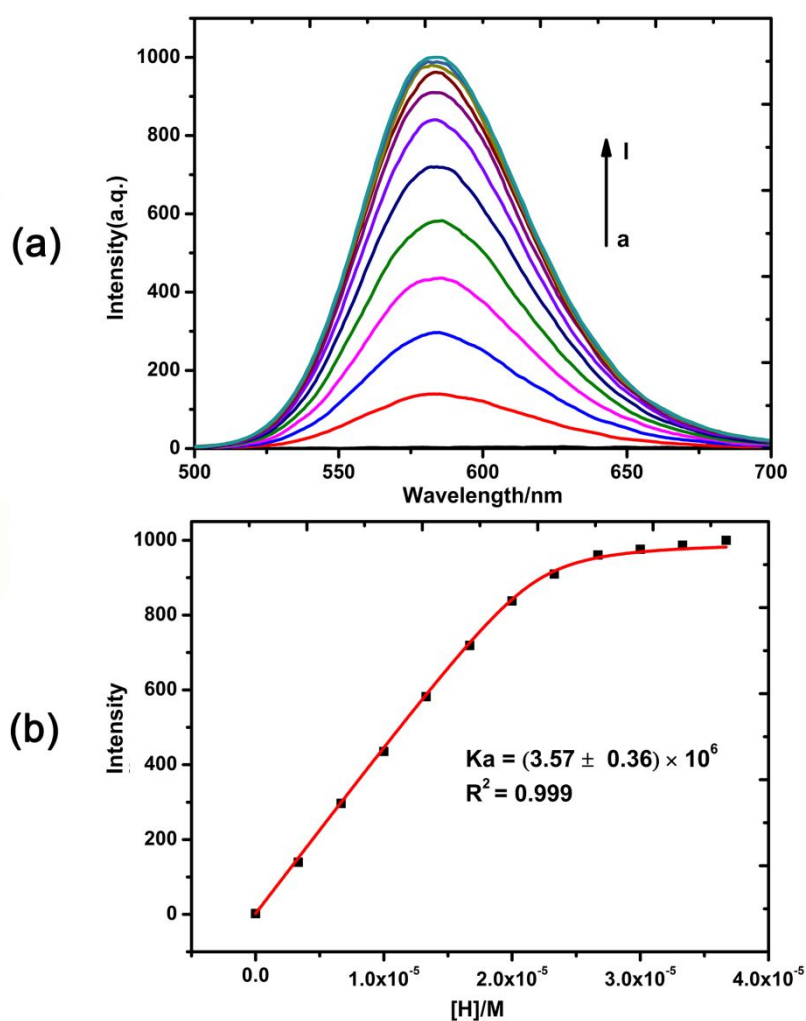


**Figure 1.** Emission spectra (a) and intensity changes of **G2** at 580 nm (b) upon the gradual addition of **H** in an aqueous solution ( $[\mathbf{G2}] = 2 \times 10^{-5} \text{ M}$ ,  $[\mathbf{H}] = 0-3.67 \times 10^{-5} \text{ M}$ ,

1  
2  
3  
4 25 °C).

5  
6  
7  
8  
9 It is known that CB[6] and **G2** guest could form an 1:1 inclusion complex with the  
10 absorbance at 450 nm and 270 times fluorescence enhancement at 580 nm.<sup>24</sup> To  
11 investigate the binding behavior between OMeCB[6] moiety of **H** and **G2**, UV-vis  
12 absorption and fluorescence experiments were further conducted. As discerned from  
13 the UV-vis absorption spectra, Job plot of OMeCB[6]/**G2** complex showed a 1:1  
14 stoichiometry by plotting the absorbance at 450 nm against the molar fraction of  
15 OMeCB[6] and **G2** (Figure S13b, Supporting Information).  
16  
17

18 For the complexation of **H** and **G2**, the stoichiometry was also determined to be 1:1  
19 based on the fluorescence intensity of **G2** in the presence of **H** (Figure S13a,  
20 Supporting Information). These results also confirmed that the guest molecule **G2**  
21 could be exclusively included into the hydrophobic cavity of OMeCB[6] in aqueous  
22 solution. Meanwhile, according to the fluorescence spectra, **G2** (20 μM) displayed  
23 very poor fluorescence with a maximum emission at 607 nm in aqueous solution,  
24 while upon addition of OMeCB[6] or **H** from 0.1 equiv. to 1.0 equiv., the emission  
25 intensity increased significantly. Additionally, a blue shift from 607 nm to 582 nm  
26 indicated the host-guest interactions between OMeCB[6] moiety and **G2** (Figure 1a,  
27 S14a). The association constant ( $K_a$ ) of **H/G2** was calculated to be  $3.57 \times 10^6 \text{ M}^{-1}$  by  
28 curve fitting method (Figure 1b). As shown in Figure S14b (Supporting Information),  
29 the  $K_a$  value for OMeCB[6]/**G2** was  $3.22 \times 10^6 \text{ M}^{-1}$ , which was in good consistence  
30 with the one in **H/G2** complexation.  
31  
32  
33  
34  
35  
36  
37  
38  
39  
40  
41  
42  
43  
44  
45  
46  
47  
48  
49  
50  
51  
52  
53  
54  
55  
56  
57  
58  
59  
60

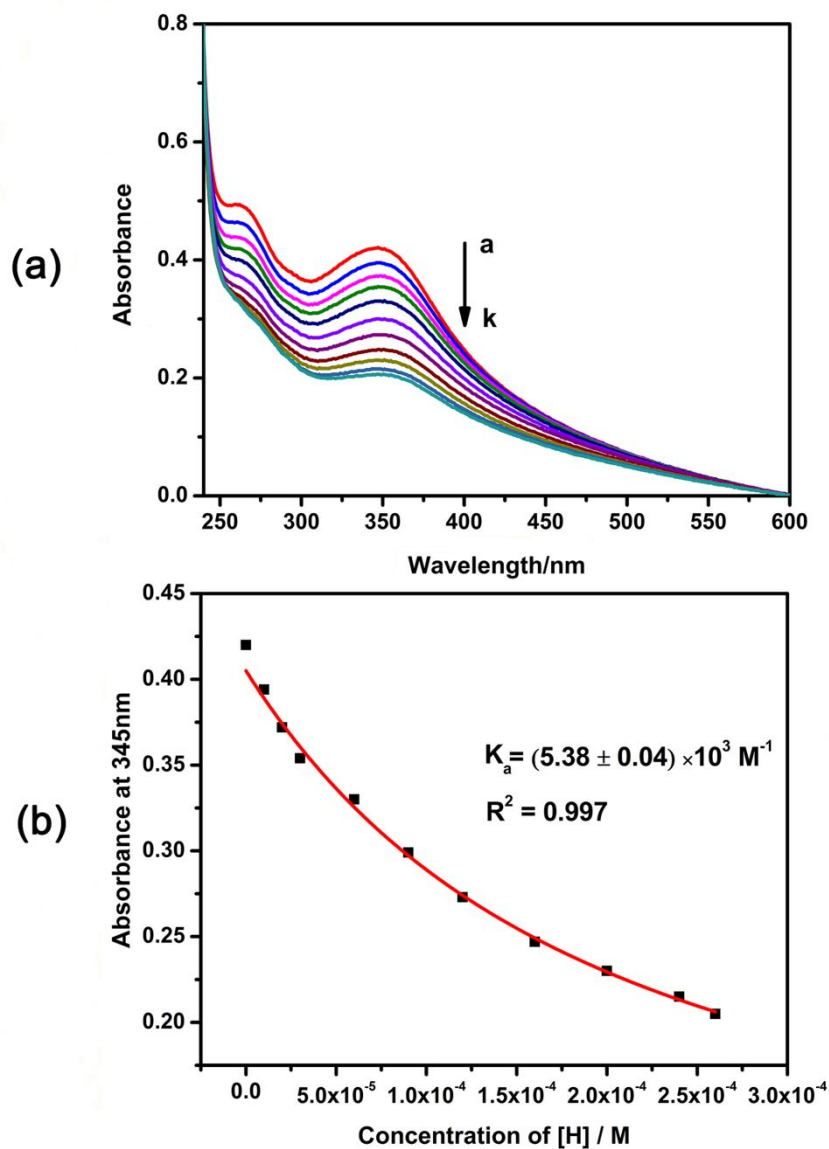


**Figure 2.** UV-vis spectra (a) and absorbance changes of **G1** at 345 nm (b) upon addition of **H** in an aqueous solution containing 3% DMSO ( $[\text{G1}] = 3.0 \times 10^{-5} \text{ M}$ ,  $[\text{H}] = 0\text{-}2.6 \times 10^{-4} \text{ M}$ , 25 °C).

It is well-known that  $\beta$ -CD could associate with adamantyl guests in aqueous solution. Then, the  $^1\text{H}$  NMR spectra was utilized by using  $\beta$ -CD and 1-adamantyl bromomethyl ketone (**ABK**) as model compound. The  $^1\text{H}$  NMR titration spectra for a fixed concentration of **ABK** upon incremental addition of  $\beta$ -CD showed the gradual

1  
2  
3  
4 downfield shifts of adamantyl protons signals (Figure S15, Supporting Information),  
5  
6 indicating the inclusion of the adamantyl moiety of **ABK** guest in the  $\beta$ -CD cavity.<sup>25</sup>  
7  
8  
9 Compared with the free  $\beta$ -CD, the <sup>1</sup>H NMR spectra also showed that upon addition of  
10  
11 1.0 equiv. of **H**, the peaks of protons H<sub>a-c</sub> on **ABK** shifted downfield significantly ( $\Delta\delta$   
12  
13 = 0.09, 0.08 and 0.22 ppm for H<sub>a-c</sub>, respectively, Figure S16, Supporting  
14  
15 Information). Meanwhile, 2D NOESY NMR spectrum of equimolar **ABK** to **H** was  
16  
17 conducted to prove the formation of host–guest complex. The NOE (nuclear  
18  
19 Overhauser enhancement) correlations were observed between adamantyl protons of  
20  
21 **ABK** and  $\beta$ -CD moiety of **H**, corroborating that adamantyl moiety was included in  
22  
23  $\beta$ -CD's cavity to form host–guest complex (Figure S17, Supporting Information).  
24  
25  
26  
27  
28  
29  
30 The host–guest complexes of **H/G1** and  $\beta$ -CD/**G1** were also studied by UV–vis  
31  
32 spectroscopy. From the absorption titration spectra, upon addition of  $\beta$ -CD to an  
33  
34 aqueous solution of **G1** with a fixed concentration, the absorbance peak at 345 nm of  
35  
36 **G1** experienced slightly red shift and the absorbance intensity was decreasing  
37  
38 gradually (Figure 2a). The binding constant for  $\beta$ -CD/**G1** complex was determined to  
39  
40 be  $(5.38 \pm 0.04) \times 10^3 \text{ M}^{-1}$  (Figure 2b). Compared to the  $\beta$ -CD/**G1** system, the  
41  
42 absorption spectra of **H/G1** showed the quite similar changes. These results revealed  
43  
44 that the adamantyl moiety of **G1** was included in the cavity of  $\beta$ -CD moiety of **H**. In  
45  
46 addition, the  $K_a$  value of **H/G1** was calculated to be  $(5.44 \pm 0.16) \times 10^3 \text{ M}^{-1}$ , which  
47  
48 was similar to the one of  $\beta$ -CD/**G2** complex (Figure S18, Supporting Information).  
49  
50  
51  
52  
53  
54  
55  
56 In addition, the spectroscopic titration experiments were also performed in D<sub>2</sub>O  
57  
58  
59  
60

1  
2  
3  
4 containing 3% DMSO, showing quite similar molecular binding behaviors (Figures  
5  
6 S19-S21, Supporting Information).  
7

8  
9 It is well known that the fluorescence emission spectrum of donor should sufficiently  
10  
11 fall into the UV-vis absorption spectra of acceptor in an effective FRET process.  
12  
13 Theoretical calculation showed that the optimized structure of the inclusion  
14  
15 complexes between **H** and two guest molecules (**G1** and **G2**) is appropriate for FRET  
16  
17 by the molecular mechanics modeling (Figure S22, Supporting Information). As can  
18  
19 be seen in Figure 3a, upon excitation at 338 nm that corresponded to absorption band  
20  
21 of the host-guest complex of **H/G1**, the 1:1 supramolecular complex of **H/G1**  
22  
23 exhibited a strong fluorescence intensity centered around 475 nm in water, which was  
24  
25 well overlapped with the absorption band of **H/G2** complex in the range of 450–550  
26  
27 nm. To further investigate the FRET process of host-guest complexes based on the  
28  
29 macrocyclic dimer, fluorescence titration experiments were conducted in  
30  
31 aqueous solution. As shown in Figure 3b, with the stepwise addition of **G2** to the  
32  
33 **H/G1** (1:1 molar ratio), the fluorescence intensity of **H/G1** was gradually decreased  
34  
35 along with the enhancement of emission of **H/G2** when excited at 338 nm. Meanwhile,  
36  
37 the color that corresponded to fluorescence emission was accordingly changed from  
38  
39 blue to yellow. In the control experiments, either **H/G2** or free **G2** barely gave  
40  
41 fluorescence emission in the same experimental conditions ( $\lambda_{\text{ex}} = 338 \text{ nm}$ ; Figure S23,  
42  
43 Supporting Information). Furthermore, the energy-transfer efficiency was calculated  
44  
45 as high as 70.3%.  
46  
47  
48  
49  
50  
51  
52  
53  
54  
55  
56  
57  
58  
59  
60

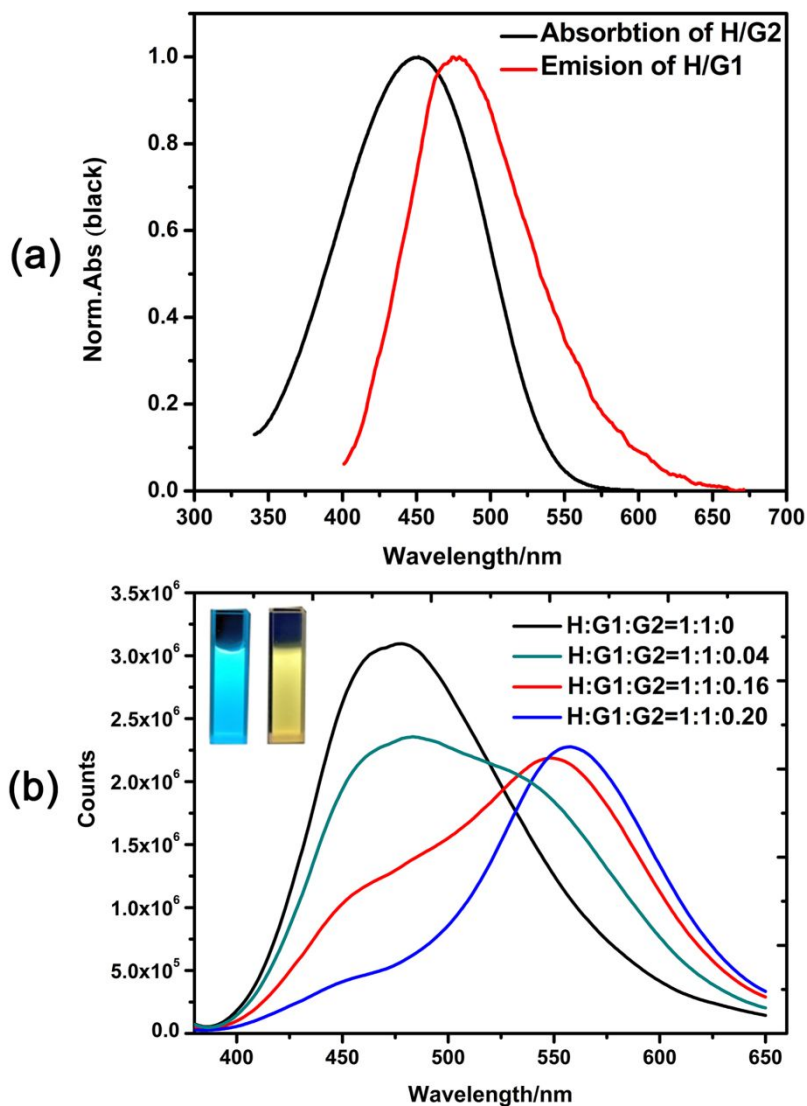


**Figure 3.** (a) Normalized absorption spectra of **H/G2** and emission spectrum of **H/G1**.

(b) Fluorescence spectra of **H/G1** ( $[\text{H}] = [\text{G1}] = 1.0 \times 10^{-4} \text{ M}$ ) in the solution of  $\text{H}_2\text{O}/\text{DMSO}$  (97:3) with different concentrations of **G2**. The concentrations of **G2** were 0,  $4.0 \times 10^{-6}$ ,  $1.6 \times 10^{-5}$ ,  $2.0 \times 10^{-5} \text{ M}$ , respectively. Inset: left, photographic images of **H/G1**, and right, **H/G1/G2** under UV light (365 nm) ( $[\text{H}] = [\text{G1}] = 1.0 \times 10^{-4} \text{ M}$ ,  $[\text{G2}] = 2.0 \times 10^{-5} \text{ M}$ ).

In conclusion, a newly macrocyclic dimer **H** bearing CD and CB moiety was synthesized via click chemistry. OMeCB[6] was chosen to construct this dimer

1  
2  
3  
4 instead of CB[6], because the solubility of parent CB[6] was rather limited in water.  
5  
6 Tetraphenylethylene modified with adamantyl moiety was synthesized to be  
7  
8 selectively trapped in the  $\beta$ -CD's cavity. After interaction with the host molecule **H**,  
9  
10 there is a strong blue emission centered at 478 nm. Then the **G2** molecule as a  
11  
12 receptor could be well encapsulated in the cavity of OMeCB[6] moiety in an aqueous  
13  
14 solution and the absorption spectrum had a good overlap with the donor emission  
15  
16 spectrum. Benefiting the good solubility of this conjugated dimeric host, a newly  
17  
18 intramolecular FRET system was constructed conveniently based on the  
19  
20 supramolecular host-guest strategy. Therefore, all the research results indicated that  
21  
22 novel macrocyclic dimer CB-CD-based host-guest complexation may be significant  
23  
24 for designing novel molecular sensors and devices and have potential application in  
25  
26 other fields such as materials and biology systems, including drug delivery, cell  
27  
28 imaging, and biosensors.  
29  
30  
31  
32  
33  
34  
35  
36  
37  
38  
39

## 40 **Experimental Section**

41  
42  
43 **Preparation of compound G1:** Compound **1**<sup>26</sup> (1.7 g, 4.86 mmol) and 1-adamantyl  
44  
45 bromomethyl ketone (1.25 g, 4.86 mmol) were dissolved in acetone (50 mL), and  
46  
47 potassium carbonate (2.02 g, 14.58 mmol) was added. The mixture was refluxed using  
48  
49 an oil bath over night. After cooling to room temperature, the solution was filtered,  
50  
51 and the filtrate was dried under reduced pressure to remove the solvent. The residue  
52  
53 was purified by column chromatography (silica gel, petroleum ether : CH<sub>2</sub>Cl<sub>2</sub> = 1:2,  
54  
55 v/v) to give compound **1** as white powder (2.42 g, 95% yield). <sup>1</sup>H NMR (400 MHz,  
56  
57  
58  
59  
60

1  
2  
3  
4 DMSO-*d*<sub>6</sub>, TMS): δ1.66 (m, 6H, H of adamantane), 1.82 (m, 6H, H of adamantane),  
5  
6 1.98 (s, 3H, H of adamantane), 4.98 (s, 2H, H of CH<sub>2</sub>), 6.60-6.62 (d, J = 8Hz, 2H, H  
7  
8 of benzene), 6.82-6.84 (d, J = 8 Hz, 2H, H of benzene) 6.93-7.18 (m, 14H, H of  
9  
10 of benzene); <sup>13</sup>C {<sup>1</sup>H} NMR (100 MHz, DMSO-*d*<sub>6</sub>, TMS): δ27.1, 35.8, 36.9, 44.5, 68.1,  
11  
12 113.7, 126.3, 127.6, 127.8, 130.5, 130.5, 130.6, 131.6, 143.3, 156.3, 208.8 ppm; MS  
13  
14 (MALDI) *m/z* : [M + H]<sup>+</sup> Calcd for C<sub>38</sub>H<sub>37</sub>O<sub>2</sub> 525.30; Found 525.34; [M + Na]<sup>+</sup> Calcd  
15  
16 for C<sub>38</sub>H<sub>36</sub>O<sub>2</sub>Na 547.26; Found *m/z* 547.31. Anal. Calcd for C<sub>38</sub>H<sub>36</sub>O<sub>2</sub>: C, 86.99; H,  
17  
18 6.92; O, 6.10. Found: C, 86.96; H, 6.90; O, 6.09.

19  
20  
21  
22  
23  
24  
25 **Preparation of compound 3:** To a solution of **2**<sup>16</sup> (30 mg, 0.027 mmol) and N,  
26  
27 N'-dihexylviologen bromide salt (13.10 mg, 0.027 mmol) in anhydrous DMSO (2  
28  
29 mL), NaH (10 mg, 0.4 mmol) was added and stirred at room temperature for 15  
30  
31 minutes. propargyl bromide (0.5 mL, 5.8 mmol) was added subsequently at 0°C and  
32  
33 the reaction mixture was stirred at room temperature for 12 hours. The reaction was  
34  
35 then diluted with 50 mL diethyl ether and filtered. The remaining solid was triturated  
36  
37 with acetone (3 × 50mL) and dried under vacuum to give a yellow solid (15 mg,  
38  
39 72%).<sup>1</sup>H NMR (400 MHz, D<sub>2</sub>O): δ 1.78 (m, 24H), 3.01 (s, H), 4.38 (m, 12H),  
40  
41 4.50-4.54 (d, J = 16 Hz, 2H), 5.55 (m, 5H), 5.70 (m, 10H); <sup>13</sup>C {<sup>1</sup>H} NMR (100 MHz,  
42  
43 D<sub>2</sub>O): δ 15.9, 16.5, 42.9, 44.0, 47.9, 48.1, 52.3, 70.8, 72.5, 77.2, 77.7, 78.0, 97.0,  
44  
45 155.7, 156.8 ppm; HRMS (MALDI) *m/z* : [M + Na]<sup>+</sup> Calcd for C<sub>47</sub>H<sub>54</sub>N<sub>24</sub>O<sub>13</sub>Na  
46  
47 1185.4200; Found 1185.4198. Anal. Calcd for C<sub>47</sub>H<sub>54</sub>N<sub>24</sub>O<sub>13</sub>: C, 48.54; H, 4.68; N,  
48  
49 28.90. Found: C, 48.52; H, 4.64; N, 28.87.

50  
51  
52  
53  
54  
55  
56  
57  
58 **Preparation of compound H:** CuI (64.48 mg, 0.34 mmol) was added to a solution of  
59  
60

1  
2  
3  
4 **3** (79.02 mg, 0.068 mmol) and **4**<sup>27</sup> (78.88 mg, 0.068 mmol) in dry DMF (10 mL), and  
5  
6 the reaction mixture was stirred at 80°C using an oil bath for 24 h under argon. After  
7  
8 cooling to room temperature, the mixture was filtered to remove any insoluble copper  
9  
10 salt, and the filtrate was evaporated under a reduced pressure to remove excess DMF.  
11  
12 The residue was purified by column chromatography (silica gel) with water/acetic  
13  
14 acid as eluent to give **H** as a white solid (101mg, yield 64%). <sup>1</sup>H NMR (400 MHz,  
15  
16 D<sub>2</sub>O): δ 1.68-1.90 (m, 24 H), 3.48-3.96 (m, 42 H), 4.25-4.52 (m, 14 H), 4.99-5.10 (m,  
17  
18 7 H), 5.52-5.77 (m, 15 H), 8.16 (s, H); <sup>13</sup>C {<sup>1</sup>H} NMR (100 MHz, D<sub>2</sub>O): δ 15.9, 16.5,  
19  
20 42.9, 44.1, 48.2, 51.4, 60.3, 70.4, 70.8, 71.8, 72.0, 72.8, 73.1, 77.8, 78.1, 81.3, 102.0,  
21  
22 156.3 ppm; MS (MALDI) *m/z* : [M + Na]<sup>+</sup> Calcd for C<sub>89</sub>H<sub>123</sub>N<sub>27</sub>O<sub>47</sub>Na 2344.796;  
23  
24 Found 2344.777. Anal. Calcd for C<sub>89</sub>H<sub>123</sub>N<sub>27</sub>O<sub>47</sub>: C, 46.02; H, 5.34; N, 16.28. Found:  
25  
26 C, 46.05; H, 5.35; N, 16.30.

27  
28  
29  
30  
31  
32  
33  
34  
35 **Supporting Information:** Detailed synthesis, characterization data, Job's plots,  
36  
37 association constant, absorption and emission spectra, <sup>1</sup>H NMR spectra and  
38  
39 theoretical calculation. This material is available free of charge via the Internet at  
40  
41 <http://pubs.acs.org>.  
42  
43  
44  
45  
46  
47

48  
49  
50  
51 **Acknowledgements.** We thank NNSFC (21432004, 21871154, 21772099, and  
52  
53 21861132001) for financial support.  
54  
55  
56  
57  
58  
59  
60

## References

- (1) (a) Lagona, J.; Mukhopadhyay, P.; Chakrabarti, S.; Isaacs, L. The Cucurbit[*n*]uril Family. *Angew. Chem. Int. Ed.* **2005**, *44*, 4844-4870; (b) Cong, H.; Ni, X.-L.; Xiao, X.; Huang, Y.; Zhu, Q.-J.; Xue, S.-F.; Tao, Z.; Lindoy, L. F.; Wei, G. Synthesis and Separation of Cucurbit[*n*]urils and Their Derivatives. *Org. Biomol. Chem.* **2016**, *14*, 4335-4364. (c) Kim, J.; Jung, I. S.; Kim, S. Y.; Lee, E.; Kang, J. K.; Sakamoto, S.; Yamaguchi, K.; Kim, K. New Cucurbituril Homologues: Syntheses, Isolation, Characterization, and X-ray Crystal Structures of Cucurbit[*n*]uril (*n* = 5, 7, and 8). *J. Am. Chem. Soc.* **2000**, *122*, 540-541; (d) McCune, J. A.; Rosta E.; Scherman, O. A. Modulating the Oxidation of Cucurbit[*n*]urils. *Org. Biomol. Chem.*, **2017**, *15*, 998-1005.
- (2) (a) Dsouza, R. N.; Pischel, U.; Nau, W. M. Fluorescent Dyes and Their Supramolecular Host/Guest Complexes with Macrocycles in Aqueous Solution. *Chem. Rev.* **2011**, *111*, 7941-7980; (b) Barrow, S. J; Kasera, S.; Rowland, M. J.; Del Barrio, J.; Scherman, O. A. Cucurbituril-Based Molecular Recognition. *Chem. Rev.* **2015**, *115*, 12320-12406; (c) Özkan, M; Kumar, Y; Keser, Y; Hadi, S. E. Tuncel, D. Cucurbit[7]uril-Anchored Porphyrin-Based Multifunctional Molecular Platform for Photodynamic Antimicrobial and Cancer Therapy. *ACS Appl. Bio Mater.* **2019**, *2*, 4693-4697.
- (3) Flinn, A.; Hough, G. C.; Stoddart, J. F.; Williams, D. J. Decamethylcucurbit[5]uril *Angew. Chem., Int. Ed. Engl.* **1992**, *31*, 1475-1477.
- (4) (a) Zhao, J.; Kim, H.-J.; Oh, J.; Kim, S.-Y.; Lee, J. W.; Sakamoto, S.; Yamaguchi, K.; Kim, K. Cucurbit[*n*]uril Derivatives Soluble in Water and Organic solvents. *Angew. Chem. Int. Ed.* **2001**, *40*, 4233-4235. (b) Wu, F.; Wu, L.-H.; Xiao, X.; Zhang, Y.-Q.; Xue, S.-F.; Tao, Z.; Day, A. I. Locating the Cyclopentano Cousins of the

- 1  
2  
3 Cucurbit[n]uril Family. *J. Org. Chem.* **2012**, *77*, 606-611.  
4  
5  
6 (5) Yu, Y.; Li, J.; Zhang, M.; Cao, L.; Isaacs, L. Hydrophobic Monofunctionalized  
7 Cucurbit[7]uril Undergoes Self-inclusion Complexation and Forms Vesicle-Type  
8 Assemblies *Chem. Commun.* **2015**, *51*, 3762-3765.  
9  
10  
11  
12 (6) Wang, X.-X.; Tian, F.-Y.; Liu, M.; Chen, K.; Zhang, Y.-Q.; Zhu, Q.-J.; Tao, Z. A  
13 Water Soluble Tetramethyl-Substituted Cucurbit[8]uril Obtained from Larger  
14 Intermediates? *Tetrahedron.* **2019**, *75*, 130488.  
15  
16  
17  
18 (7) Jon, S. Y.; Selvapalam, N.; Oh, D. H.; Kang, J. K.; Kim, S. Y.; Jeon, Y. J.; Lee, J.  
19 W.; Kim, K. Facile Synthesis of Cucurbit[n]uril Derivatives via Direct  
20 Functionalization: Expanding Utilization of Cucurbit[n]uril. *J. Am. Chem. Soc.* **2003**,  
21 *125*, 10186-10187.  
22  
23  
24  
25 (8) Shetty, D.; J. K.; Park, K. M.; Kim K. Can We Beat the Biotin–Avidin Pair?:  
26 Cucurbit[7]uril-Based Ultrahigh Affinity Host–Guest Complexes and Their  
27 Applications. *Chem. Soc. Rev.* **2015**, *44*, 8747-8761.  
28  
29  
30  
31 (9) Kaifer, A. E. Toward Reversible Control of Cucurbit[n]uril Complexes. *Acc.*  
32 *Chem. Res.* **2014**, *47*, 2160-2167.  
33  
34  
35  
36 (10) Sun, C.; Zhang, H.; Li, S.; Zhang, X.; Cheng, Q.; Ding, Y.; Wang, L.-H.; Wang,  
37 R. Polymeric Nanomedicine with “Lego” Surface Allowing Modular  
38 Functionalization and Drug Encapsulation. *ACS Appl. Mater. Interfaces* **2018**, *10*,  
39 25090-25098.  
40  
41  
42  
43 (11) Liu, J.; Lan, Y.; Yu, Z. Tan, C. S. Y.; Parker, R. M.; Abell, C.; Scherman, O. A.  
44 Cucurbit[n]uril-Based Microcapsules Self-Assembled within Microfluidic Droplets: A  
45 Versatile Approach for Supramolecular Architectures and Materials. *Acc. Chem. Res.*  
46 **2017**, *50*, 208-217.  
47  
48  
49  
50 (12) Elbashir, A. A.; Hassan, A. E.; Crit, Y. Supramolecular Analytical Application of  
51  
52  
53  
54  
55  
56  
57  
58  
59  
60

1  
2  
3 Cucurbit[*n*]urils Using Fluorescence Spectroscopy. *Rev. Anal. Chem.* **2015**, *45*, 52-61.

4  
5 (13) Park, K. M.; Hur, M. Y.; Ghosh, S. K.; Boraste, D. M.; Kim, S.; Kim, K.

6  
7 Cucurbit[*n*]uril-Based Amphiphiles That Self-Assemble into Functional

8  
9 Nanomaterials for Therapeutics. *Chem. Commun.* **2019**, *55*, 10654-10664.

10  
11 (14) Ayhan, M. M.; Karoui, H.; Hardy, M.; Rockenbauer, A.; Charles, L.; Rosas, R.;

12  
13 Udachin, K.; Tordo, P.; Bardelang, D.; Ouari, O. Comprehensive Synthesis of

14  
15 Monohydroxy-Cucurbit[*n*]urils (*n* = 5, 6, 7, 8): High Purity and High Conversions. *J.*

16  
17 *Am. Chem. Soc.* **2015**, *137*, 10238-10245.

18  
19 (15) Ayhan, M. M.; Karoui, H.; Hardy, M.; Rockenbauer, A.; Charles, L.; Rosas, R.;

20  
21 Udachin, K.; Tordo, P.; Bardelang, D.; Ouari, O. Correction to “Comprehensive

22  
23 Synthesis of Monohydroxy-Cucurbit[*n*]urils (*n* = 5, 6, 7, 8): High Purity and High

24  
25 Conversions”. *J. Am. Chem. Soc.* **2016**, *138*, 2060-2060.

26  
27 (16) Shen, F.-F.; Chen, K.; Zhang, Y.-Q.; Zhu, Q.-J.; Tao, Z.; Cong, H. Mono-and

28  
29 Dihydroxylated Symmetrical Octamethylcucurbiturils and Allylated Derivatives. *Org.*

30  
31 *Lett.* **2016**, *18*, 5544-5547.

32  
33 (17) Wang, X. -X.; Chen, K.; Shen, F.-F.; Wang, Y.; Zhang, Y.-Q.; Tao, Z.; Cong, H.

34  
35 Mono - , Di - , and Tri - Hydroxylated Symmetrical Hexamethylcucurbit[3,3]uril and

36  
37 Allylated Derivatives. *Eur. J. Org. Chem.* **2017**, *2017*, 6980-6985.

38  
39 (18) (a) Lou, X.-Y.; Song, N.; Yang, Y.-W. Fluorescence Resonance Energy Transfer

40  
41 Systems in Supramolecular Macrocyclic Chemistry. *Molecules* **2017**, *22*, 1640; (b)

42  
43 Yesilgul, N.; Seven, O.; Guliyev, R.; Akkaya, E. U. Energy Harvesting in a

44  
45 Bodipy-Functionalized Rotaxane. *J. Org. Chem.* **2018**, *83*, 13228-13232; (c) Guo, S. ;

46  
47 Song, Y.; He, Y.; Hu, X.-Y.; Wang, L. Highly Efficient Artificial Light - Harvesting

48  
49 Systems Constructed in Aqueous Solution Based on Supramolecular Self - Assembly.

50  
51 *Angew. Chem. Int. Ed.* **2018**, *57*, 3163-3167.

- 1  
2  
3 (19) Sun, J.; Hua, B.; Li, Q.; Zhou, J.; Yang, Acid/Base-Controllable FRET and  
4 Self-Assembling Systems Fabricated by Rhodamine B Functionalized  
5 Pillar[5]arene-Based Host–Guest Recognition Motifs. *J. Org. Lett.* **2018**, *20*, 365-368.  
6  
7  
8  
9  
10 (20) Li, M.; Lee, A.; Kim, K. L.; Murray, J.; Shrinidhi, A.; Sung, G.; Park, K. M.;  
11 Kim, K. Autophagy Caught in the Act: A Supramolecular FRET Pair Based on an  
12 Ultrastable Synthetic Host–Guest Complex Visualizes Autophagosome–Lysosome  
13 Fusion. *Angew. Chem. Int. Ed.* **2018**, *57*, 2120-2125.  
14  
15  
16  
17  
18 (21) Zhao, Q.; Liu, Y. Tunable Photo-Luminescence Behaviors of  
19 Macrocyclic-Containing Polymer Networks in the Solid-State. *Chem. Commun.* **2018**,  
20  
21  
22  
23  
24  
25  
26  
27 (22) Li, J.-J.; Chen, Y.; Yu, J.; Cheng, N.; Liu, Y. A Supramolecular Artificial  
28 Light-harvesting System with Ultrahigh Antenna Effect. *Adv. Mater.* **2017**, *29*,  
29  
30  
31  
32  
33 (23) (a) Branná, P.; Černochová, J.; Rouchal, M.; Kulhánek, P.; Babinský, M.; Marek,  
34 R.; Nečas, M.; Kuřitka, I.; Vícha, R. Cooperative Binding of Cucurbit[*n*]urils and  
35  $\beta$ -Cyclodextrin to Heteroditopic Imidazolium-Based Guests. *J. Org. Chem.* **2016**, *81*,  
36  
37  
38  
39  
40  
41  
42  
43  
44  
45  
46  
47  
48  
49  
50  
51  
52  
53  
54  
55  
56  
57  
58  
59  
60

1  
2  
3 1401-1407.  
4  
5

6 (25)(a) Zhang, Y.-M.; Liu, Y.-H.; Liu, Y. Cyclodextrin-Based  
7  
8 Multistimuli-Responsive Supramolecular Assemblies and Their Biological Functions.  
9

10  
11 *Adv. Mater.* **2019**, 1806158; (b) Fu, H.-G.; Chen, Y.; Yu, Q.; Liu, Y. A  
12  
13 Tumor-Targeting Ru/Polysaccharide/Protein Supramolecular Assembly with High  
14  
15 Photodynamic Therapy Ability. *Chem. Commun.* **2019**, 55, 3148-3151.  
16  
17

18 (26) Sun, J.; Shao, L.; Zhou, J.; Hua, B.; Zhang, Z.; Li, Q.; Yang, J. Efficient  
19  
20 Enhancement of Fluorescence Emission via TPE Functionalized Cationic Pillar [5]  
21  
22 arene-Based Host–Guest Recognition-Mediated Supramolecular Self-Assembly  
23  
24 *Tetrahedron Lett.* **2018**, 59, 147-150.  
25  
26

27 (27) Sun, H.-L.; Chen, Y.; Han, X.; Liu, Y. Tunable Supramolecular Assembly and  
28  
29 Photoswitchable Conversion of Cyclodextrin/Diphenylalanine-Based 1D and 2D  
30  
31 Nanostructures. *Angew. Chem. Int. Ed.*, **2017**, 56, 7062-7065.  
32  
33  
34  
35  
36  
37  
38  
39  
40  
41  
42  
43  
44  
45  
46  
47  
48  
49  
50  
51  
52  
53  
54  
55  
56  
57  
58  
59  
60